

MASTERPRE-EQUILIBRIUM DECAY PROCESSES IN ENERGETIC
HEAVY ION REACTIONSMARSHALL BLANN
Lawrence Livermore National Laboratory,
Livermore, California, U.S.A.

Abstract The Boltzmann master equation (BME) is defined for application to precompound decay in heavy ion reactions in the 10-100 MeV/nucleon regime. Predicted neutron spectra are compared with measured results for central collisions of ^{20}Ne and ^{12}C with ^{163}Ho target nuclei. Comparisons are made with subthreshold π^0 yields in heavy ion reactions between 35 and 84 MeV/nucleon, and with the π^0 spectra. The BME is found to be an excellent tool for investigating these experimentally observed aspects of non-equilibrium heavy ion reactions.

INTRODUCTION

Many precompound decay phenomena have been and are being observed in heavy ion reactions in the energy regime above 8-10 MeV/nucleon. I wish to explore the applications of the Boltzmann master equation (BME) to the interpretation of some of the observable quantities. The BME will be seen to be a physically transparent, highly tractable, semi-classical model for following relaxation processes in nuclear reactions which may be described as being dominated by two body (nucleon-nucleon) processes. We will therefore be considering reasonably central collision processes, anticipating that peripheral processes lead to reactions (e.g., fragmentation) less likely describable as projectile coalescence followed by a series of two body relaxation interactions.

I would like to summarize the main elements of the physics of the BME model and the formulation. Then, I would like to discuss the most crucial and least well understood part of the model, the assumed injection of

jeu

H. M. BLANN

nucleons during coalescence. Next, I will show some of the aspects of heavy ion reactions which may be investigated in either a time dependent or time integrated frame, and compare results of BME calculations with experimental neutron spectra and with subthreshold pion production cross sections and spectra. Finally, I shall offer suggestions for future experimental measurements and state our conclusions.

PHYSICAL ASSUMPTIONS AND FORMULATION

PHYSICAL ASSUMPTIONS AND CONSIDERATIONS

The physics we require in our model includes the following:

- A. Energy transfer mediated by two body (nucleon-nucleon) collisions. Cross sections given by free $c_{nn}(E)$, $c_{pp}(E)$, $c_{pn}(E)$; these must be modified in turn by the Pauli exclusion principle.
- B. The calculation must be time dependent, following both fusion (coalescence) and post-fusion periods.
- C. The relaxation process must have competition between N-N scattering and continuum emission. During coalescence, there must be a source term for injection of nucleons and excitation energy into the system, in addition to internal scattering and continuum emission.

For this, we use a modification of the BME as encoded for nuclear reactions by George Harp, and as originally described by Harp, Miller and Berne.¹ We next qualitatively and then quantitatively describe this model approach as modified for HI reactions.

The reactions are followed in the BME in an energy space only, and not in a geometric or momentum space. Thus, angular information is removed in the simplifying assumptions used in the formulation, although this could be replaced in an a-posteriori fashion as it is in exciton type models. The BME idea is represented in Fig. 1, where it may be seen that for a given energy bin in the nuclear potential, we calculate explicitly the rates of scattering into, out of, and continuum emission from the bin of interest. Therefore, the time evolution of the nucleon energy population is followed explicitly. The population

PRE-EQUILIBRIUM DECAY PROCESSES...

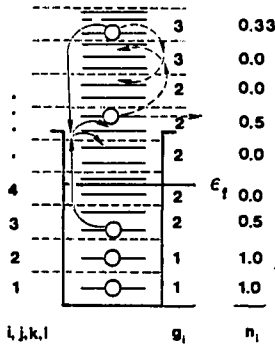


FIGURE 1. Representation of a Fermi gas nucleus as treated in the Boltzmann master equation. The nucleus is divided into 1 MeV wide energy bins, indexed by i, j, k or l counting from the bottom of the Fermi sea. The number of single particle levels, \$g_i\$ per MeV is calculated, and the occupation probability \$n_i\$ is also followed. The rate of scattering into and out of each bin (and if energetically allowed, of emission into the continuum) is calculated for a time interval less than the nucleon-nucleon collision period; all nucleon populations are appropriately modified after each time interval. The Pauli exclusion principle is treated by the \$(1-n_i)\$ terms (Eq. 1).

readjustment versus time is mediated solely by two body N-N collision processes based on free N-N scattering cross-sections and the Pauli exclusion principle. The set of master equations may be represented by:²

(Eq. 1)

$$\begin{aligned} \frac{dn_i}{dt} = & \sum_{\mu} [\omega_{\mu}^{\downarrow} g_{\mu}^{\downarrow} n_{\mu}^{\downarrow} (1-n_i^{\downarrow}) - \omega_{\mu}^{\uparrow} g_{\mu}^{\uparrow} n_i^{\downarrow} (1-n_{\mu}^{\downarrow})] - [\omega_{\mu}^{\downarrow} g_{\mu}^{\downarrow} n_i^{\downarrow} (1-n_{\mu}^{\downarrow}) - \omega_{\mu}^{\uparrow} g_{\mu}^{\uparrow} n_{\mu}^{\downarrow} (1-n_i^{\downarrow})] \\ & + \sum_{\mu} [\omega_{\mu}^{\downarrow} g_{\mu}^{\downarrow} n_i^{\downarrow} n_{\mu}^{\downarrow} (1-n_i^{\downarrow}) - \omega_{\mu}^{\uparrow} g_{\mu}^{\uparrow} n_i^{\downarrow} (1-n_{\mu}^{\downarrow})] + \omega_{\mu}^{\downarrow} g_{\mu}^{\downarrow} n_i^{\downarrow} (1-n_{\mu}^{\downarrow}) - \omega_{\mu}^{\uparrow} g_{\mu}^{\uparrow} n_{\mu}^{\downarrow} (1-n_i^{\downarrow}) \\ & - n_i^{\downarrow} \omega_{\mu}^{\downarrow} g_{\mu}^{\downarrow} (e_i^{\downarrow} - e_{\mu}^{\downarrow} + B_{\mu}), \quad i = 1, \dots, e_i^{\downarrow} + E^*, \quad i = 1, \dots, E^* - B_{\mu} + X + Y, \end{aligned}$$

where X is a term similar to the first summation with superscript "p", replaced by a superscript "n", and Y is a time dependent source term representing nucleons injected during the fusion process.

The Pauli exclusion operators may be seen in the BME as the $(1-n_i)$ terms, giving the fraction empty of final bins. The symbols of the BME are summarized in Table 1. The rate of scattering of two nucleons at energies i and j into final energies k and l is given by:

(Eq. 2)

$$\omega_{ij \rightarrow kl}^{pp} = \frac{\sigma^{pp}(e_i^p + e_j^p) [(2/M)(e_i^p + e_j^p)]^{1/2}}{V \sum_{mn} g_m^2 g_n^2 \sigma^{pp}(e_i^p + e_j^p - e_m^p - e_n^p)}$$

where an average collision angle of 90° is assumed. A more thorough discussion of the BME, as encoded originally by Harp, Miller, and Berne, and later modified by Blann, may be found in Refs. 1 and 2.

There is still the question of the rate and energy distribution of interacting nucleons during coalescence in a heavy ion reaction. How to calculate and model this is a very interesting, very much open question. In the limit of a light projectile on a heavy target we might expect a random, energy conserving distribution, with degrees of freedom $(n-1)$ approximately equal to or greater than the projectile mass, A_p . A larger value than A_p might be anticipated since nucleons might be exchanged between both target and projectile during fusion, and further there may be collective degrees of freedom relevant to these reactions. If the number of degrees of freedom could be determined for the fusing system, we could use the Ericson distribution function to find the partition of energy for $(n-1)$ degrees of freedom with every energy partition having equal a-priori probability:³

$$N(E) = \frac{(gE)^{n-1}}{p!h!(n-1)!} \quad (\text{Eq. 3})$$

where E is the excitation energy, g the (assumed constant) single particle level density, p the number of excited particles, h the number of holes and $n=p+h$.

PRE-EQUILIBRIUM DECAY PROCESSES...

One way of testing this notion is by using the BME with an initial exciton population given by the Ericson distribution, with the initial exciton number n taken as a free parameter,⁴ selected to give a best fit to experimental fusion gated spectra. This has been done by the Berlin^{5,6} and Zagreb groups.⁷ Results are summarized in Fig. 2, based on a figure from Refs. 6 and 7, where values of n from A_p-1 to A_p+8 were found for a very wide range of projectiles. The narrow range of n values tends to support the basic idea that the reactions may be described as proceeding through a number of degrees of freedom closely associated with the projectile mass. The early data seemed to show a strong energy dependence of the value extracted for the n parameter; however, note in Fig. 2 that the recent 25 MeV/nucleon ^{12}C point of the Berlin group⁶ implies a more nearly constant value of n . Indeed, we will show that we can satisfactorily fit all the Berlin Ne and 25 MeV/nucleon ^{12}C results satisfactorily with $n=A_p$ and with no modification of the nucleon-nucleon mean free paths.

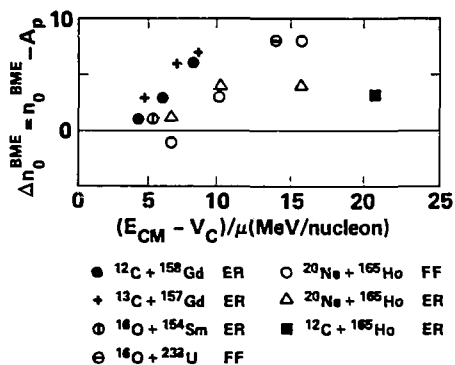


FIGURE 2. Degrees of freedom deduced for several heavy ion induced reactions by varying the n parameter in the BME. This figure is taken from Refs. 10 and 11. The ordinate gives the difference between the best fit n parameter of the Ericson expression as used for the initial exciton distribution in the BME injection term, and the projectile mass number A_p . The abscissa gives the projectile

H. M. BLANN

energy in MeV/nucleon (c_m) above the coulomb barrier. The choices of target and projectile are given in the legend. Sources of original data are given in Ref. 6.

The course comparisons of n in Fig. 2 are encouraging, and we owe thanks to the Berlin and Zagreb groups for exploring this important parameter of the BME approach; the onus is now on us to put more physics into the coalescence distribution function. For example, including higher partial waves than $l=0$ will tend to reduce the energy dependence noted for the n parameter. Similarly, the distribution function should be limited to maximum and minimum nucleon energies as given by the relative and Fermi velocities (as is done for calculation of the π^0 production cross sections discussed in III.C). Accessible cells in phase space rather than equipartition based on energy should also be considered. We are looking into these possibilities at present, and hope to have results in the near future.

Next, we investigate the time dependent relaxation decay information available from the BME, and compare the BME using the Ericson input distribution function with experimental (HI, n) spectra. This will be followed by comparisons with predictions for π^0 production, for which case the distribution function must be calculated with constraints on maximum nucleon energies.

COMPARISONS OF CALCULATED AND EXPERIMENTAL RESULTS

TIME DEPENDENT RESULTS OF BME

The decay characteristics predicted by the master equation are displayed graphically in Fig. 3 for the $Al+Kr$ system for the assumption of 27 initial excitons. The graphs in Fig. 3 show many of the predicted decay properties versus time for the example shown; characteristics of proton emission are similar to neutron emission.

The time at which the infusion of nucleons from the projectile to the composite system is complete is indicated in Fig. 3(b). Determining the approximate time at which a given system has equilibrated is more subjective. We have taken the results in Fig. 3(b) and extrapolated the linear regions of the curves at long times to shorter times. The region first showing an acceleration in the

PRE-EQUILIBRIUM DECAY PROCESSES...

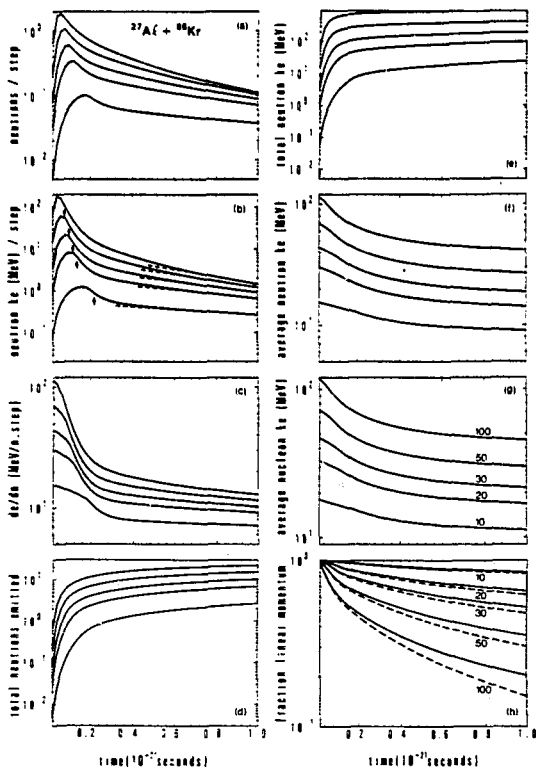


FIGURE 3. Calculated precompound decay quantities versus time for reactions induced by 10, 20, 30, 50, and 100 MeV/ nucleon (c.m.) ^{27}Al ions on ^{86}Kr . For each bombarding energy, the figure shows the following versus time: (a) the number of neutrons emitted during each time step ($\Delta t=2 \times 10^{-23}$ sec) of the computation; (b) the kinetic energy removed by neutrons during each Δt ; (c) the energy per neutron removed during each Δt [i.e., the quotient of (b) by (a)]; (d) the total neutrons emitted up to

H. M. BLANN

time t ; (e) the total kinetic energy removed by neutrons up to time t ; (f) the average neutron energy of all neutrons emitted up to time t ; (g) the average nucleon (neutron plus proton) kinetic energy removed up to time t ; and (h) the fraction linear momentum remaining on the heavy residues up to time t . In (b) the up arrows indicate the time at which fusion was complete for each incident energy; the intersections of the dashed lines with the calculated curves were used to estimate an equilibration time. The incident energies are shown in (g) and (h). The ordering shown in (g) is valid for (a)-(g). In (h) the dashed curves represent the calculated linear momentum if it is assumed that all nucleons are emitted at 0° to the beam, i.e., if the angular correction $RAC \approx h/k$ is not made.

rate of neutron emission is taken as the equilibration time. Dashed curves have been added in Fig. 3(b) to illustrate this procedure.

The figure shows a rapid increase of precompound decay as projectile energies exceed 10 MeV/nucleon, as predicted earlier.^{3,4} The systems may be seen to relax rapidly toward equilibrium following the conclusion of coalescence, i.e., in periods of the order of $2-5 \times 10^{-22}$ sec. Nonetheless, these periods are in the range of the collective times required to go from contact to an equilibrium composite configuration (particularly in the "extra" push region), and from the compound shape to saddle. Many nucleons may be emitted during this time, considerably altering both the excitation energy and angular momentum of the hot, equilibrated residue. For example, for Al+Kr at 100 MeV/nucleon, our model calculation predicts approximately 35 nucleons (and probably additional d, t, α , etc., clusters) removed during this short period, and 1800 of the 2700 MeV of maximum available excitation removed. Interpretation of, e.g., coincident fission fragments in such an experiment would therefore suggest an analysis in terms of a much cooler fissioning system, and of significantly lower mass, than given by the composite system mass and c.m. projectile energy. Precompound decay of nucleons should become of major importance as projectile energies go beyond 30 MeV/nucleon, and it is predicted to be a very significant process at somewhat lower energies.

PRE-EQUILIBRIUM DECAY PROCESSES...

(HI,n) Spectra

In Fig. 4 we show comparisons between evaporation residue (ER) and fission fragment (FF) gated, angle integrated neutron spectra from the ^{20}Ne bombardment of ^{165}Ho .

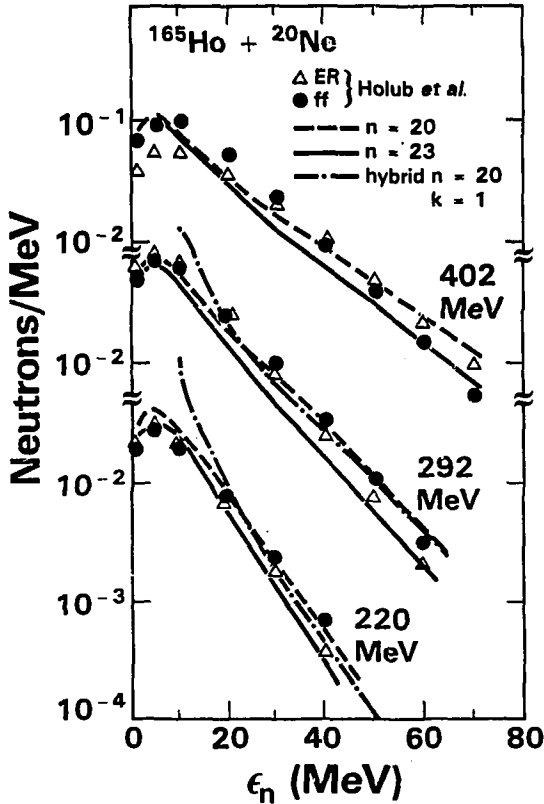


FIGURE 4. Calculated and experimentally deduced spectra for the $^{165}\text{Ho}(^{20}\text{Ne},n)$ reaction at laboratory energies of 220, 292, and 402 MeV. Experimental

H. M. BLANN

points from Ref. 5 result from an integration of a moving source fit to experimental yields for the fast component only. Experimental yields were gated on evaporation residues (ER) as represented by open triangles, and on fission fragments (FF) shown by closed circles. Calculated results are shown for the BME with n of the Ericson expression (Eq. 3) taken as 20 and 23, and for a hybrid model calculation with $n=20$.

The "experimental results" are parameterized calculated points for the "fast" component. These data were fitted by the Berlin group with the BME with n values of 20-24 (ER gated spectra) and 20-28 (FF gated spectra) with the average nucleon mean free path being twice the result due to N-N scattering processes. We show calculated results for these spectra using $n=20$ and 23 without modification of the nucleon mfp.² The value of $n=20$ seems to give a satisfactory fit to all the data, within the uncertainties stated previously on the "primal" distribution function used, and somewhat even based on uncertainties in the angle integration method used on the data. I should emphasize that the absolute values of the calculated spectra are compared with the experimental results in Fig. 4 without any normalization, and are all calculated without adjustment of the nucleon-nucleon mean free path.

Recently the Berlin group has measured $^{165}\text{Ho}(^{12}\text{C},n)$ at 25 MeV/nucleon incident energy.⁶ Results are shown in Fig. 5. They found excellent agreement with experimental spectra with $n=15$, $k=4$, as shown. We get satisfactory agreement for $n=12$, $k=1$. The BME may be seen to give a quite satisfactory agreement for an a-priori calculation over a broad range of incident energies and projectiles, yielding spectra correct in shape and magnitude, without normalization of the spectral intensities.

In Figs. 4 and 5, we also see the result of a calculation using the hybrid model via the code ALICE.^{4,8} Here too, for $k=1$ and $n=A_p$, the calculated spectra are in quite good agreement with the experimentally deduced results. The disagreement at lower channel energies results because the ALICE calculation includes equilibrium components, while the experimental representation has excluded these. This precompound calculation is essentially the one suggested in 1974 before the experiments could be performed.⁴

PRE-EQUILIBRIUM DECAY PROCESSES...

The BME seems to give a reasonable representation of the nucleonic cascade. Could the linear momentum removed by the nucleons account for the linear momentum decrement observed in many experiments? This can be calculated if we know something of the angular distribution of the emitted nucleons.

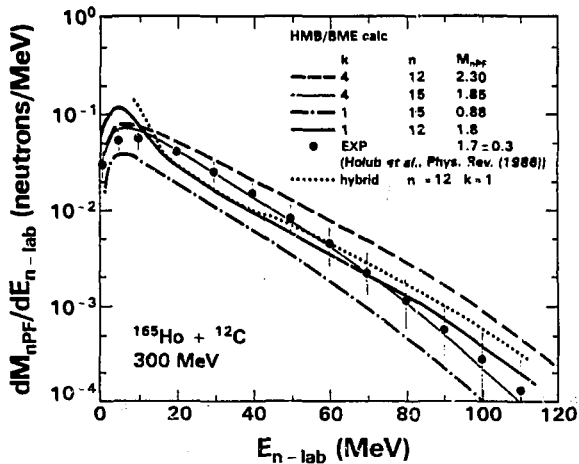


FIGURE 5. Calculated and experimentally deduced neutron spectra for the $^{165}\text{Ho} (^{12}\text{C},n)$ reaction at 25 MeV/nucleon. The data were angle integrated as for Fig. 4; these results are from Ref. 6. Several spectra calculated with the BME in Ref. 6 are shown. To these, we have added results of the BME for $n=12, k=1$ (mean free path multiplier), and a result with the hybrid model from code ALICE for $n=12, k=1$.

Linear Momentum Transfer

Rather than performing a sophisticated calculation of nucleon angular distributions, or better yet, inputting algorithms based on experimental results, we have assumed nucleon emission at an energy dependent angle based on a

H. M. BLANN

Heisenberg type of limit,

$$R\Delta\theta \geq \hbar/k \quad , \quad (\text{Eq. 4})$$

a result based on earlier work of Mantzouranis, et al.⁹ This algorithm was shown to be useful in the case of (N, N') angular distributions.¹⁰ Eventually, a more sophisticated approach should be taken. Nonetheless, this limit should give a rough estimate of the momentum removed by the nucleonic cascade. Results of momentum transfer calculations for $^{16}\text{O}+^{60}\text{Ni}$ and $^{27}\text{Al}+^{86}\text{Kr}$ are shown in Fig. 6. Some experimental results, due to many workers,

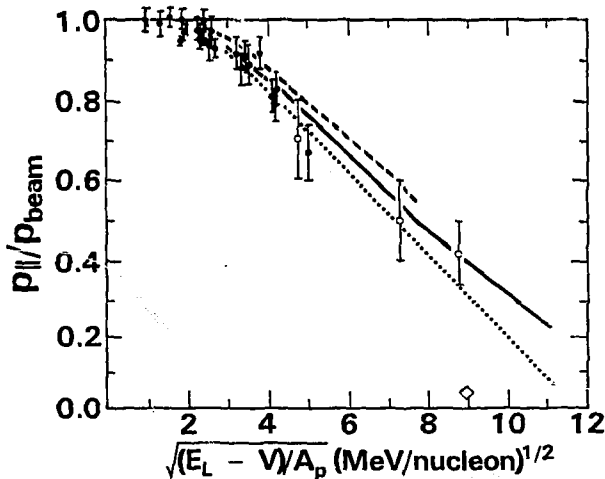


FIGURE 6. Calculated and experimental results for the fraction of beam linear momentum transferred ($p_{||}/p_{\text{beam}}$) in heavy ion reactions versus laboratory velocity in excess of the coulomb barrier. The experimental values shown are from a compilation due to Yuen-Dat Chan (Ref. 11). The dotted curve is a calculated BME result for $^{60}\text{Ni}+^{16}\text{O}$ assuming $n=16$, with a lower limit of nucleon injection energy above ϵ_f of $(\sqrt{\epsilon_R} - \sqrt{\epsilon_f})^2$. The solid line is for $^{60}\text{Ni}+^{16}\text{O}$ assuming $n=19$, and the

PRE-EQUILIBRIUM DECAY PROCESSES...

dashed line is for $^{27}\text{Al}+^{86}\text{Kr}$ assuming $n=30$. The dotted and solid curves differ from results in Ref. 2 in that the distribution functions used had both upper and lower limit constraints on the injection energy.

as summarized by Chan, et al.,¹¹ are also shown. Overall, the agreement between calculated and experimental results is quite good, but there are some very big caveats. First, in a more detailed comparison at the lower incident energy end of the curve, Viola finds that the BME overestimates the linear momentum decrement.¹² Secondly, there is some evidence that at the higher bombarding energies, a significant part of the linear momentum decrement may be due to cluster emission. While our calculation makes a small allowance for this, some experiments suggest that nature may be providing many more clusters per interaction.¹³ The only reason for hedging this statement at all is that some of these experimental measurements have instrumental cutoffs of the low energy protons, so that a proper estimate of cluster vs. nucleon emission multiplicities is still somewhat ambiguous.

Perhaps this is a good point to emphasize that linear momentum transfer is not a very unambiguous probe of models such as the BME. Rather the ER or FF gated nucleon or cluster emission spectra provide a more stringent test. For the available nucleon emission data the BME is doing well for relatively few data; what is needed is a broader data base. Measurement of the very high energy end of the nucleon spectra would be especially interesting, particularly as it relates to the assumed mechanism of coupling nucleon relative momenta with Fermi momenta in the injection/coalescence process. This point is in turn of particular interest to N-N collision explanations for subthreshold pion production. In this regard, the ($^{12}\text{C},n$) data of Fig. 5 are particularly interesting, for they show the presence of high energy nucleons capable of producing pions via the N-N collision process.

Subthreshold Pion Production

Early on, Bertsch¹⁴ suggested that the Fermi momentum and relative nucleon motion might couple in heavy ion reactions to give nucleons sufficient energy to produce pions via a N-N collision mechanism. Arndt and VerWest have tabulated excitation functions for $N+N \rightarrow N+N + \text{pion}$.¹⁵ We should be able to add these channels to the

H. M. BLANN

BME to probe the possibility of the N-N collision process as a viable subthreshold pion production mechanism.¹⁶ The input nucleon spectra for these calculations have been calculated with all energy partitions equally likely, but with no exciton having more than $(\sqrt{\epsilon_f} + \sqrt{\epsilon_r})^2$ units of energy where ϵ_f is the projectile Fermi energy and ϵ_r is the relative per nucleon energy of approach.¹⁶ We assumed $n=A_p$ which, recalling the recent Berlin results (Fig. 5), gave excellent agreement between calculated and measured nucleon spectra in the pion production energy range. The rate equations for pions may be represented by:¹⁶

(Eq. 5)

$$\begin{aligned} \frac{dN^\pi}{dt} = & \sum_{ijk'l'm} \omega_{ij}^{\pi p0} g_{-k'l'm} g_m g_l^2 g_j^2 n_l^n n_j^n (1-n_k^n)(1-n_l^n) \\ & + \sum_{ijk'l'm} \omega_{ij}^{\pi n0} g_m g_l^2 g_j^2 n_l^n n_j^n (1-n_k^n)(1-n_l^n) \\ & + \sum_{ijk'l'm} \omega_{ij}^{\pi n\pi0} g_m g_l^2 g_j^2 n_l^n n_j^n (1-n_k^n)(1-n_l^n), \end{aligned}$$

with the collision rate expressions given by:¹⁶

(Eq. 6)

$$\omega_{ij}^{\pi p0} = \frac{\sigma^{\pi p0}(\epsilon_i + \epsilon_j) [(2/M)(\epsilon_i^2 + \epsilon_j^2)]^{1/2}}{V \sum_{\alpha \beta p} g_\alpha g_\beta g_p \delta(\epsilon_i^2 + \epsilon_j^2 - \epsilon_\alpha^2 - \epsilon_\beta^2 - \epsilon_p^2 - m_\pi^2)}$$

Results of these calculations via the BME for a fairly broad range of experimentally measured systems are summarized in Table 2. The calculated yields include a crude π^0 emission attenuation factor estimated for a 2 Fm mean free path. More details may be found in Ref. 16. The results are also quite sensitive to the value of the Fermi energy assumed for the projectile, which was 35 MeV in all cases. We might, for example, expect lower values for the lightest projectiles. In view of the uncertainties of these calculations, we subjectively feel that agreement within a factor of 3-4 between calculated and measured yields is confirmation that the N-N collision is one (but by no means the only) viable mechanism for subthreshold pion production. This is seen to be the case for all the

PRE-EQUILIBRIUM DECAY PROCESSES...

systems summarized in Table 2, except $^{40}\text{Ca}+^{40}\text{Ar}$, where the discrepancy is a factor of five.

Pion spectra from the Boltzmann master equation are compared with experimental results in Fig. 7. The calculated results are seen to be too hard compared with experimental spectra. However, the higher energy pions would be more likely to interact through the Δ resonance,

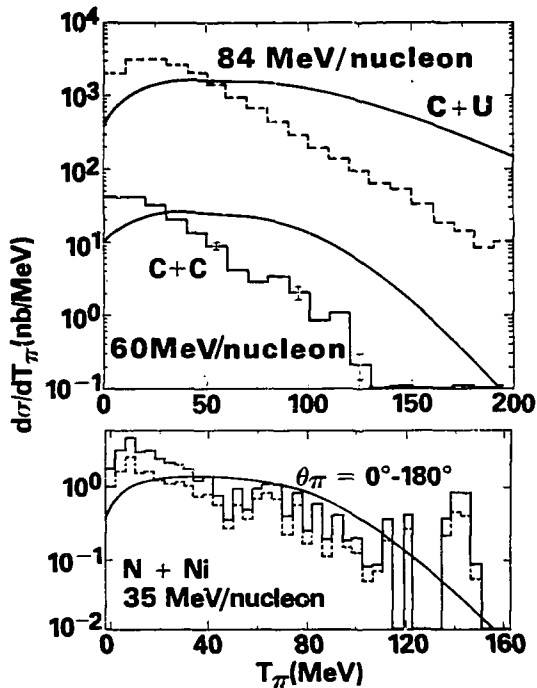


FIGURE 7. Calculated and experimental π^0 spectra for 35 MeV/nucleon ^{14}N on ^{58}Ni (lower), for 60 MeV/nucleon $^{12}\text{C}+^{12}\text{C}$ (center) and 84 MeV/nucleon $^{12}\text{C}+^{238}\text{U}$ (top).

H. M. BLANN

and this would tend to soften the spectrum of observed pions. The disagreement in spectral shape is therefore qualitatively in the proper direction.

It is interesting to compare the time dependence of the nucleon vs. π^0 emission rates in Fig. 8. The π^0 rate is extremely sensitive to the very early time history of the reaction, and to the source nucleon energy distribution, in marked contrast to the nucleon decay.

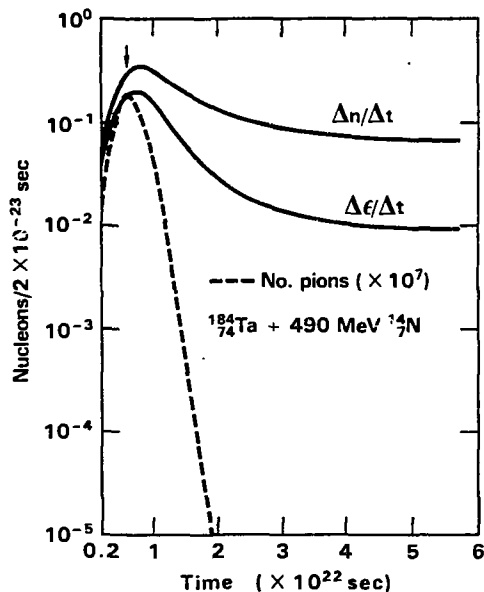


FIGURE 8. Calculated π^0 , neutron emission, and neutron de-excitation rates versus time from the Boltzmann master equation. The down arrow shows the time at which coalescence is considered to be complete in the BME. These results are for $^{184}\text{W} + 490 \text{ MeV } ^{14}\text{N}$. The rate of energy loss is on a relative scale on the ordinate. The ordinate gives pion or nucleon emission rates per time unit of 2×10^{-23} sec.

PRE-EQUILIBRIUM DECAY PROCESSES...

CONCLUSIONS

The BME (and hybrid model) are transparent in the physics used to treat the equilibration process, specifically, a series of N-N collisions generated by free scattering cross-sections and the Pauli exclusion principle. The BME, in particular, is very versatile and it is easy to use to test ideas; e.g., pion production cross-sections, incomplete momentum transfer. The model works quite well in reproducing nucleon emission spectra for central collision processes using an input distribution based on $n \approx A_p$. More work needs to be done in modeling the initial distribution function with the coupling constraints, phase space constraints, and with consideration of angular momentum averaging.

A broader range (projectile and projectile energy variations) of nucleon and cluster emission spectra gated on central collisions would be welcome as a more severe test of the BME and other precompound decay models. Measurement of nucleons at the highest kinetic energies may give crucial information on the microscopic details of the coalescence process, in particular the coupling of the relative motion and Fermi motion of the projectile nucleons, and of the viability of the N-N collision process for subthreshold pion production.

All caveats considered, these simple precompound decay models yield a wealth of insight into the dynamics of heavy ion reactions. Many of the predictions made as early as 1974 by use of these models⁴ are now being realized in experimental measurements. These models should continue to be valuable tools in the interpretation of heavy ion induced precompound decay reactions.

H. M. BLANN

REFERENCES

1. G. D. Harp, J. M. Miller and B. G. Berne, Phys. Rev. 165, 1166 (1968); G. D. Harp and J. M. Miller, Phys. Rev. C 3, 1847 (1971).
2. M. Blann, Phys. Rev. C 23, 205 (1981); C 31, 1245 (1985).
3. T. E. O. Ericson, Adv. Phys. 9, 423 (1960).
4. M. Blann, Nucl. Phys. A 235, 211 (1974); M. Blann, "Proceedings of the International School on Nuclear Physics," Predeal, Romania 1974, ed. A. Ciocanel, p. 249, Bucharest (1976); M. Blann, A. Mignerey and W. Scobel, Nukleonika 21, 335 (1976).
5. E. Holub, et al., Phys. Rev. C 28, 252 (1983).
6. E. Holub, et al., Phys. Rev. C 33, 143 (1986).
7. N. Cindro, M. Korolija and E. Holub, "Fundamental Problems in Heavy Ion Collisions," ed. by N. Cindro, et al., p. 301, World Scientific, Singapore (1985).
8. M. Blann, Phys. Rev. Lett. 27, 337 (1971).
9. G. Mantzouranis, H. A. Weidenmuller and D. Agassi, Z. Phys. A 276, 145 (1976).
10. M. Blann, W. Scobel and E. Plechaty, Phys. Rev. C 30, 1493 (1984).
11. Y. D. Chan, et al., Phys. Rev. C 27, 447 (1983).
12. C. B. Chitwood, et al., Phys. Rev. Lett. 55, 1376 (1985).
13. J. L. Laville, et al., Phys. Lett. 156B, 42 (1985); T. C. Awes, et al., Phys. Rev. C 24, 89 (1981).
14. G. F. Bertsch, Phys. Rev. C 15, 713 (1977).
15. B. J. VerWest and R. A. Arndt, Phys. Rev. C 25, 1979 (1982).
16. M. Blann, Phys. Rev. C 32, 1231 (1985).

PRE-EQUILIBRIUM DECAY PROCESSES...

17. J. Stachel, et al., in "Proceedings of the Institute for Nuclear Studies," RIKEN Symposium on Heavy Ion Physics, Tokyo, Japan, 1984 (unpublished).
18. H. Noll, et al., Phys. Rev. Lett. 52, 1284 (1984).

DISCLAIMER

This report was prepared as an account of work sponsored by an agency of the United States Government. Neither the United States Government nor any agency thereof, nor any of their employees, makes any warranty, express or implied, or assumes any legal liability or responsibility for the accuracy, completeness, or usefulness of any information, apparatus, product, or process disclosed, or represents that its use would not infringe privately owned rights. Reference herein to any specific commercial product, process, or service by trade name, trademark, manufacturer, or otherwise does not necessarily constitute or imply its endorsement, recommendation, or favoring by the United States Government or any agency thereof. The views and opinions of authors expressed herein do not necessarily state or reflect those of the United States Government or any agency thereof.

This work was performed under the auspices of the U. S. Department of Energy by the Lawrence Livermore National Laboratory under contract No. W-7405-Eng-48.

DISCLAIMER

This report was prepared as an account of work sponsored by an agency of the United States Government. Neither the United States Government nor any agency thereof, nor any of their employees, makes any warranty, express or implied, or assumes any legal liability or responsibility for the accuracy, completeness, or usefulness of any information, apparatus, product, or process disclosed, or represents that its use would not infringe privately owned rights. Reference herein to any specific commercial product, process, or service by trade name, trademark, manufacturer, or otherwise does not necessarily constitute or imply its endorsement, recommendation, or favoring by the United States Government or any agency thereof. The views and opinions of authors expressed herein do not necessarily state or reflect those of the United States Government or any agency thereof.